Carbohydrate Polymers 93 (2013) 698–708

Contents lists available at SciVerse ScienceDirect

Carbohydrate Polymers

journal homepage: www.elsevier.com/locate/carbpol

Processing of microcrystalline cellulose in dimethyl sulfoxide, urea and supercritical carbon dioxide

Aniket Selarka[a,1], Ronald Baney[a,*], Siobhan Matthews[b]

[a] Department of Materials Science and Engineering, University of Florida, Gainesville, FL, USA
[b] SCF Processing Ltd, Drogheda, Ireland

ARTICLE INFO

Article history:
Received 1 June 2012
Received in revised form
22 November 2012
Accepted 30 November 2012
Available online 28 December 2012

Keywords:
Cellulose
Supercritical carbon dioxide
Urea
Crystallinity
Hydrogen bond
Infrared spectroscopy

ABSTRACT

Efficient utilization of cellulose in polymer blends is limited because of its high crystallinity. In this work, an attempt to change the inherent crystallinity of cellulose was performed by exposing it to two systems viz. dimethyl sulfoxide (DMSO)–supercritical CO_2 and DMSO–urea–supercritical CO_2. The cellulose samples processed in DMSO–supercritical CO_2 system at 2500 psi, 3500 psi, and 4500 psi showed a reducing trend of the relative crystallinity with increasing pressure. The reduction in the relative crystallinity occurred due to weakening of inter-chain hydrogen bonds in cellulose. The cellulose samples were processed in DMSO–urea–supercritical system at 2500 psi and 4500 psi. A maximum 55% reduction in relative crystallinity was found in the sample that contained 1.80 mol fractions of urea and processed at 2500 psi. This reduction in crystallinity was due to the presence of a DMSO–urea complex, which caused weakening of intermolecular hydrogen bond and an intramolecular hydrogen bond.

1. Introduction

There is a growing demand to develop products from bio-based materials and use technologies that can untie the broad dependence on fossil fuels and non-renewable resources. Increasing awareness to minimize plastic waste accumulation in landfills and soil has triggered attempts toward utilizing bio-based materials over conventional polymeric materials. Usage of non-biodegradable polymers especially the ones derived from petroleum resources can be reduced by replacing them completely or a part of them (by blending) with natural bio-polymers such as polysaccharides and natural polypeptides. Among bio-polymers, cellulose and starch are the most important natural polysaccharides (Briassoulis, 2004). Cellulose, being the most abundant natural polysaccharide and renewable biomass, represents about 1.5×10^{12} tons of the total biomass produced annually (Klemm, Heublein, Fink, & Bohn, 2005). The high crystallinity of cellulose makes it an excellent filler material to impart strength to a polymer blend. However, because of the closely packed-highly crystalline structure formed due to hydrogen bonds, it cannot be chemically processed easily (Yin et al., 2007). As a result, the efficient utilization of cellulose in making fully or partially biodegradable polymer products is still a challenging task.

For cellulose based polymer blends, a good balance of properties can be achieved if the crystallinity of cellulose is reduced and/or the compatibility with a base polymer is improved. This can also lead to use of high volume of cellulose in polymer blends, which will not only form a suitable alternative to starch but will also not affect the human food chain unlike the way that the use of starch could potentially do. Generally, physical properties of cellulose are changed by derivatization (Edgar et al., 2001) which involves chemical modification of the cellulose structure, usually by functionalizing the polymer chains using a solvent. In this research, emphasis has been given on the study of changes in crystallinity and molecular structure of cellulose when it was processed under a combination of non-hazardous and environmentally benign solvent systems viz. DMSO– supercritical CO_2 or DMSO–urea–supercritical CO_2. The primary objective of this research was to explore such solvent systems to reduce crystallinity of microcrystalline cellulose and develop understanding of micro-structural changes occur therein.

1.1. Structure and properties of cellulose

Cellulose is a polymer, which is biogenetically formed by two repeat units of D-glucopyranose molecules that are linked through

Abbreviations: CO_2, carbon dioxide; DMSO, dimethyl sulfoxide; DRIFT, diffused reflectance infrared Fourier transform spectroscopy; NMR, nuclear magnetic resonance; P_c, critical pressure; T_c, critical temperature; WAXRD, wide angle X-ray diffraction.

* Corresponding author. Present address: 168 Rhines Hall, Materials Science and Engineering, University of Florida, Gainesville, FL 32611, USA. Tel.: +1 352 846 3785.
E-mail address: rbane@mse.ufl.edu (R. Baney).
[1] Present address: 6476 NE Alder Street, Apt # A, Hillsboro, OR 97124, USA.

0144-8617/$ – see front matter © 2013 Elsevier Ltd. All rights reserved.
http://dx.doi.org/10.1016/j.carbpol.2012.11.101

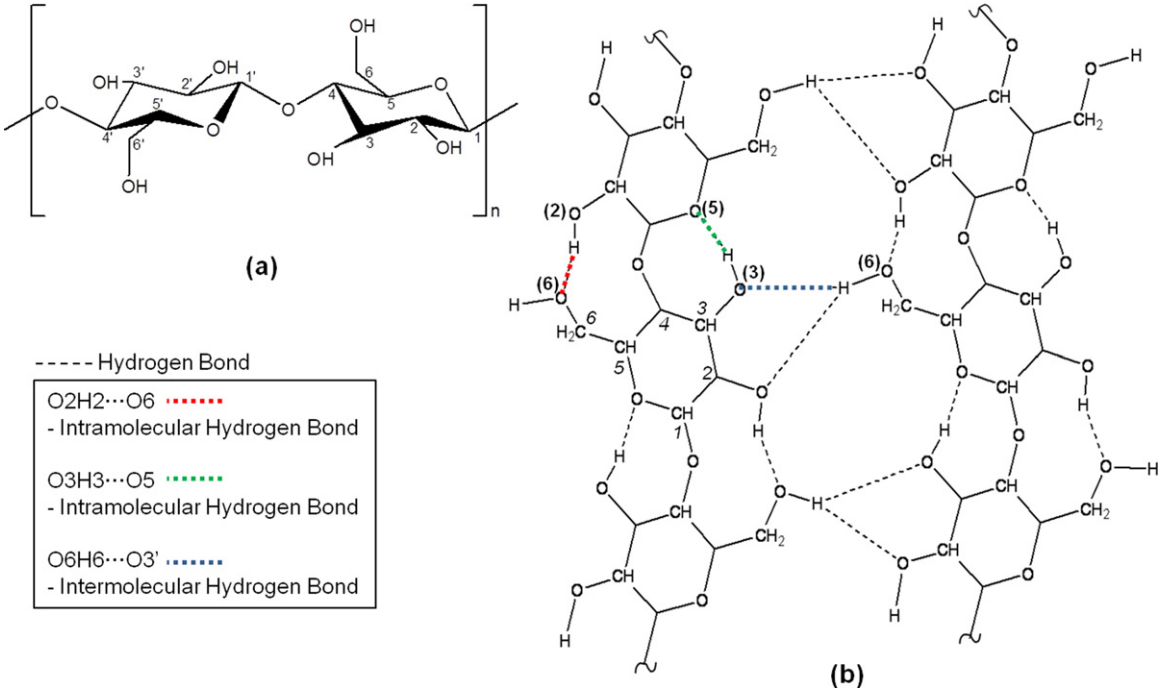

Fig. 1. Intra-chain and inter-chain hyderogen bonding in Cellulose I (Klemm, Schmauder, et al., 2005; O'Sullivan, 1997).

covalent β-glycosidic bonds between C1 and C4 carbon atoms. The glucopyranose ring adopts a chair conformation 4C1. Three OH groups per anhydroglucose unit (AGU) are present at C2, C3, and C6 in equatorial positions. Every second AGU ring is rotated by 180° in the plane in order to accommodate preferred bond angles of acetal oxygen bridges (Fig. 1a). The presence of oxygen atoms on both β-glycosidic bond and pyranose ring and hydroxyl groups forms a three dimensional semi-crystalline supermolecular structure via ordered intra-chain and inter-chain hydrogen bonding (Ilharco, Garcia, Lopes da Silva, & Vieira Ferreira, 1997; Klemm, Heublein, et al., 2005; Klemm, Schmauder, & Heinze, 2005; Kondo, Sawatari, Manley, & Gray, 1994; Kovalenko, 2010; O'Sullivan, 1997). The extensive inter-molecular and intra-molecular hydrogen bonding between chains (Fig. 1b) results in large lattice forces which causes high crystallinity and water insolubility (Kondo et al., 1994; Scott, 2002).

1.2. Characteristics and properties of supercritical fluids

Supercritical fluids are clean and versatile alternatives to the traditional organic solvents. These can be used to either replace the organic solvents or collect and recycle the organic solvents after its use in many chemical processes (Wen, Jiang, & Zhang, 2009). Zheng et al. defined supercritical fluid as "a fluid that is in a gaseous form but compressed at temperatures above its critical point to a liquid like density" (Zheng, Lin, & Tsao, 1998). Characteristics like high diffusivity, high mass transfer rates, low viscosity, low surface tension, and high solvency (Leitner, 1999; Wypych, 2001) make supercritical fluids an excellent solvent for synthesis and processing of micro to nano-scale substances (Johnston & Shah, 2004). Among supercritical fluids, supercritical carbon dioxide meets the criteria of ecological and economical constraints very well. Supercritical carbon dioxide is non-toxic, non-flammable, inexpensive, readily available, and has lower critical temperature and pressure than other supercritical fluids (Kjellow & Henriksen, 2009; Zheng et al., 1998; Zheng & Tsao, 1996). Carbon dioxide does not create any chemical waste and it is also a green house component (Schacht, Zetzl, & Brunner, 2008). The supercritical fluid state of CO_2 is formed beyond critical temperature (T_c = 304 K) and critical pressure (P_c = 7.3 MPa) (Kazarian, 2000).

2. Experiment strategies

Dimethyl sulfoxide is a biodegradable, non-toxic polar solvent. Its high dipole moment (Aminabhavi & Gopalakrishna, 1995) and it hydrogen bond forming properties with cellulose (Fernandez Cid et al., 2007) can be used to expand the micro-fibrillar structure of cellulose. Carbon dioxide in its supercritical state displays dual properties – solvating power of liquid and mass transfer properties of a gas (Taherzadeh & Karimi, 2008). Such characteristics in combination with properties of DMSO can be used to disrupt and re-orient the molecular bonds in cellulose. Microcrystalline cellulose can first be swollen by solvent DMSO and then pressurized under supercritical CO_2 to improve effectiveness of DMSO toward altering the microstructure. DMSO is soluble in supercritical CO_2 at convenient processing conditions (Rajasingam, Lioe, Pham, & Lucien, 2004; Vega Gonzalez, Tufeu, & Subra, 2002). Application of pressurized CO_2 can help the solvent molecules penetrate deeper into crystalline structure, cause disruption of hydrogen bonds, and finally lead to reduction in crystallinity (Fig. 2). High mass-transfer rate in the supercritical state can assist the diffusion of the solvent molecules. DMSO can later be extracted from cellulose by depressurizing CO_2 over a fixed pressure range.

Sudden change in CO_2 pressure during DMSO extraction may cause collapsing of cellulose chains and reformation of the hydrogen bonds, which may lead to only limited reduction in crystallinity. The reformation of hydrogen bonds in cellulose can be restricted by incorporating small quantities of a compatible compound. Urea is a low cost- natural compound. It is also capable of forming hydrogen bonds with cellulose (Nada, Kamel, & El-Sakhawy, 2000; Yin et al., 2007). Urea is easily soluble in DMSO (Markarian, Gabrielyan, & Grigoryan, 2004) but poorly soluble in supercritical CO_2 (Catchpole et al., 2005). According to our hypothesis, DMSO can act as a carrier for urea molecules in crystalline structure of cellulose. Supercritical CO_2 can assist in diffusing urea deeper into the structure. The poor solubility of urea with supercritical CO_2 can be used to extract

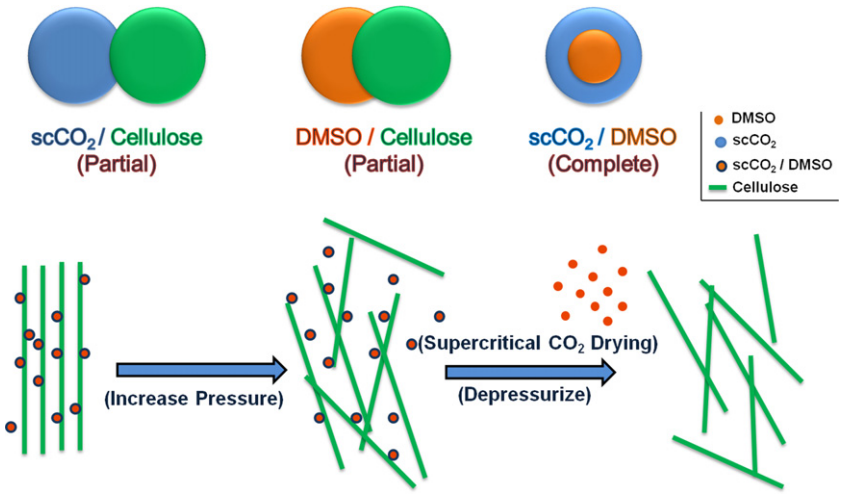

Fig. 2. Reaction strategy.

only DMSO during the depressurization run. In this way, urea can be introduced into cellulose structure to reduce the cellulose crystallinity. Urea could either interact chemically with cellulose by forming cellulose carbamate (Nada et al., 2000) or it can physically be entrapped in cellulose structure. Either way it will increase the free volume of cellulose and so contribute in reducing crystallinity. The selective interactions among the components are summarized in Table 1 (Catchpole et al., 2005; Fernandez Cid et al., 2007; Krässig, 1993; Markarian et al., 2004; Rajasingam et al., 2004; Vega Gonzalez et al., 2002).

3. Experimental

3.1. Materials

Microcrystalline cellulose Avicel® FD100 provided by FMC Corporations, Philadelphia, PA was used as the starting material. The supplier claimed that the molecular weight was about 36,000 g/mol and degree of polymerization is approximately 140. The crystallinity index is approximately 82% and particle size falls in the range of 6–12 μm. Dimethyl sulfoxide (DMSO) A.C.S. grade was purchased from Fisher Scientific, Atlanta, GA and used as received. Urea A.C.S. grade (U-15) was also received from Fisher Scientific Co. CO_2 gas cylinder was purchased from Airgas South Inc., Gainesville, FL.

3.2. Experiment procedure

For each batch reaction, 1.5 g microcrystalline cellulose was added into 5 ml DMSO and the mixture was stirred at 80 rpm at 30 °C for 2 min inside the fume hood. The white heterogeneous solution, as formed, was immediately transferred into the view cell before a gel formed. For batch reactions with urea, known quantity of urea was first added into 5 ml DMSO, stirred at 80 rpm at 30 °C (303.15 K) until a clear homogeneous solution was formed. A fixed amount of cellulose was added subsequently. The view cell was held horizontally using a Stir-Plate support and purged with CO_2 between 50 and 80 psi (0.3–0.5 MPa) for about 1 min. The view cell was heated to 80 °C (353 K). During the heating process, outlet port of the view cell was closed and it was filled with CO_2 at 850 psi (5.8 MPa) when the temperature reached to about 40 °C (313 K). The inlet port of the view cell was closed and CO_2 was pressurized to desired pressure values of 2500 psi (17.3 MPa), 3500 psi (24.1 MPa) or 4500 psi (31.0 MPa) by the syringe pump. Once the temperature reached the set value, the inlet port of the view cell was opened and pressurized CO_2 was transferred into it at gas flow rate of 80 ml/min. The inlet valve for the view cell was closed when syringe pump and the view cell came to pressure equilibrium. The solution was kept inside the view cell under this temperature and pressure condition for 30 min. The solution was stirred at about 500 rpm using a stirring bar inside the view cell. The stirring speed was controlled by a Stir-Plate. After 30 min reaction time DMSO was removed along with CO_2 by depressurizing the CO_2. The depressurization process was conducted in multiple steps of 2500 psi (17.3 MPa) to 2000 psi (13.8 MPa). If the batch reaction was conducted at a CO_2 pressure higher than 2500 psi then the depressurization process included a first step down from maximum pressure to 2500 psi and 2500 psi to 2000 psi subsequent multiple pressure steps. Depressurization was stopped when the sample under the view cell was observed as a free flowing powder. Finally, the pressure and temperature were brought down to room conditions. The sample was removed from view cell and transferred to a closed container.

It is worth to note that the batch reactions involving both microcrystalline cellulose and urea required longer depressurization times to obtain dry powder samples compared to reactions in absence of urea. The compositions and processing conditions used are listed in Tables 2 and 3 below.

4. Characterization

A wide angle X-ray diffraction (WAXRD) study was performed using an X-ray diffractometer (Philips APD 3720). The XRD was conducted using CuKα radiation at 40 kV and 20 mA. The wavelength of the X-ray was 1.54 Å. Diffraction patterns were collected in the 2θ range of 5–40° at step size of 0.02. The diffraction results were treated and analyzed by deconvoluting the spectra into 5 separate peaks in the 2θ range of 10.77–31.77° using ProFit software. The relative degree of crystallinity was calculated by subtracting

Table 1
Miscibility among cellulose/DMSO/urea/supercritical CO_2.

	Cellulose–DMSO	Cellulose–supercritical CO_2	DMSO–supercritical CO_2	DMSO–urea	Urea–supercritical CO_2
Miscibility of components	Partial (only swells)	Poor	Good	Good	Poor

Table 2
Compositions and batch processing conditions for cellulose/DMSO/supercritical CO_2.

Identification	Cellulose (g)	DMSO (ml)	Temperature (°C)	CO_2 pressure (psi)
Unmodified cellulose	1.5	N/A	N/A	N/A
D2500	1.5	5	80	2500
D3500	1.5	5	80	3500
D4500	1.5	5	80	4500

amorphous region from crystalline region. The amorphous region was represented by a broad peak with highest intensity at $2\theta = 22.8°$, which was generated by first selecting a peak at 2θ value of 19° and then applying Pearson VII profile fit until a best fit was obtained.

Diffused reflectance infrared spectroscopy was obtained by a Thermo Electron Magna 760, Thermo Scientific Inc., MA. Approximately 0.003 g of sample was first mixed with 0.3 g of potassium bromide (KBr) in a high speed shaker for 1 min. Microcrystalline cellulose Avicel® FD100 was kept in an oven for 24 h at 80 °C before preparing the sample for spectroscopy. The spectra were recorded at 4 cm^{-1} resolution in the range of 400 cm^{-1} to 4000 cm^{-1}. The number of scans for each sample was set at 64. The spectra were further analyzed by performing curve-fitting simulations using an open source – peak fitting software 'fityk 0.9.4'. The bands for the hydrogen bonding region (3000–3800 cm^{-1}) were deconvoluted assuming peaks as Gaussian, with a number of iterations to get the good fit (Mishra, Chattopadhyay, Sreedhar, & Raju, 2006). The R^2 values were visually observed but not recorded for each measurement. In general, the R^2 range was observed to be varying from 0.75 to 0.90 for all of the Gaussian fits. A series of fitting iterations were carried out until a noticeable improvement in the Gaussian curve that overlapped the data points was obtained. In this work the visual observation of 'how well' the data points are covered under the Gaussian curve formed the basis of calling it a good fit.

5. Results and discussion

5.1. Microcrystalline cellulose processed with DMSO–supercritical CO_2

5.1.1. WAXRD analysis

Crystalline peaks in the cellulose diffraction spectra arise from crystal lattices formed due to glycosidic bonds, hydrogen bonds and van der Waals dispersion forces in the macromolecule (Bansal, Hall, Realff, Lee, & Bommarius, 2010). Crystal microfibrils are made of both crystalline and amorphous regions (Garvey, Parker, & Simon, 2005). These regions in microcrystalline cellulose Avicel® FD100, separated by using fityk tool, are depicted in Fig. 3. The assignment of crystalline planes to the peaks was based on previous reports (Bansal et al., 2010; Park, Baker, Himmel, Parilla, & Johnson, 2010). The relative degree of crystallinity of cellulose was calculated by using the following formula (Focher et al., 2001; Zhang et al., 2009; Zhou, Zhang, & Guo, 2005):

$$\text{relative crystallinity } (\%) = \left(\frac{A_c}{A_a + A_c}\right) \times 100$$

where A_c is the sum of integral area of peaks assigned to crystalline regions $(1\bar{1}0)$, (110), (102), (200) and A_a is the integral area of amorphous region as shown by broad curve joining the end points of the spectrum with maximum intensity at about $2\theta = 22.5°$. WAXRD spectra of cellulose samples processed under DMSO and supercritical CO_2 at pressures ranging from 2500 psi to 4500 psi were compared with unmodified cellulose (Fig. 3). It was found that the crystal structure of cellulose did not change due to the processing but the (200) peak intensity was reduced and the amorphous region was increased with increasing processing pressure of supercritical CO_2. This could be due to breaking down of cellulose crystallites. The relative crystallinity of samples followed a decreasing trend with increasing processing pressure. Cellulose processed with DMSO at 2500 psi (D2500) was only marginally affected but relative crystallinity of cellulose processed with DMSO at 4500 psi (D4500) was reduced by more than 45% from that of unmodified cellulose. From these results, it can be concluded that an increase in the processing pressures of supercritical CO_2 must have resulted in deeper penetration of DMSO into micro-fibrils of cellulose, but it did not have a very significant effect on the original crystal structure. The change in relative crystallinity in spite of unmodified crystal structure suggests that the DMSO molecules affected the cellulose mostly by interacting with intermolecular bonds in the amorphous region of cellulose whereas high pressure supercritical CO_2 aided in breaking the cellulose crystallites.

5.1.2. DRIFT analysis

Cellulose macromolecule has three different hydroxyl groups that participate in inter-chain and intra-chain hydrogen bonding. Combination of these hydrogen bonded OH stretching vibrations show a broad IR peak in 3000–3600 cm^{-1} region (Kondo et al., 1994). Heavy overlapping of inter-chain and intra-chain hydrogen bonds in OH stretch region makes the interpretation of corresponding bands difficult. Various authors have separated these bands but the assignment of hydrogen bonds corresponding to the peak positions varies not only with author's discretion but also with the source of cellulose (Kokot, Czarnik-Matusewicz, & Ozaki, 2002; Maréchal & Chanzy, 2000; Oh et al., 2005; Sugiyama, Persson, & Chanzy, 1991; Watanabe, Morita, & Ozaki, 2006).

The infrared spectra of cellulose – as received, and cellulose processed under supercritical CO_2 at 2500 psi, 3500 psi, and 4500 psi pressures are shown in Fig. 4. It can be seen that the hydrogen bonding region (3000–3600 cm^{-1}) became narrow with increase in supercritical CO_2 pressure. This change can be attributed to disruption in hydrogen bonding either due to fewer hydroxyl groups to form hydrogen bond (Kondo et al., 1994) or change in the

Table 3
Compositions and batch processing conditions for cellulose/DMSO/urea/supercritical CO_2.

Identification	Cellulose (g)	DMSO (ml)	Urea (g)	CO_2 pressure (psi)	Temperature (°C)
UD25025	1.5	5	0.25	2500	80
UD25050	1.5	5	0.50	2500	80
UD25075	1.5	5	0.75	2500	80
UD25010	1.5	5	1.0	2500	80
UD45025	1.5	5	0.25	4500	80
UD45050	1.5	5	0.50	4500	80
UD45075	1.5	5	0.75	4500	80
UD45010	1.5	5	1.0	4500	80

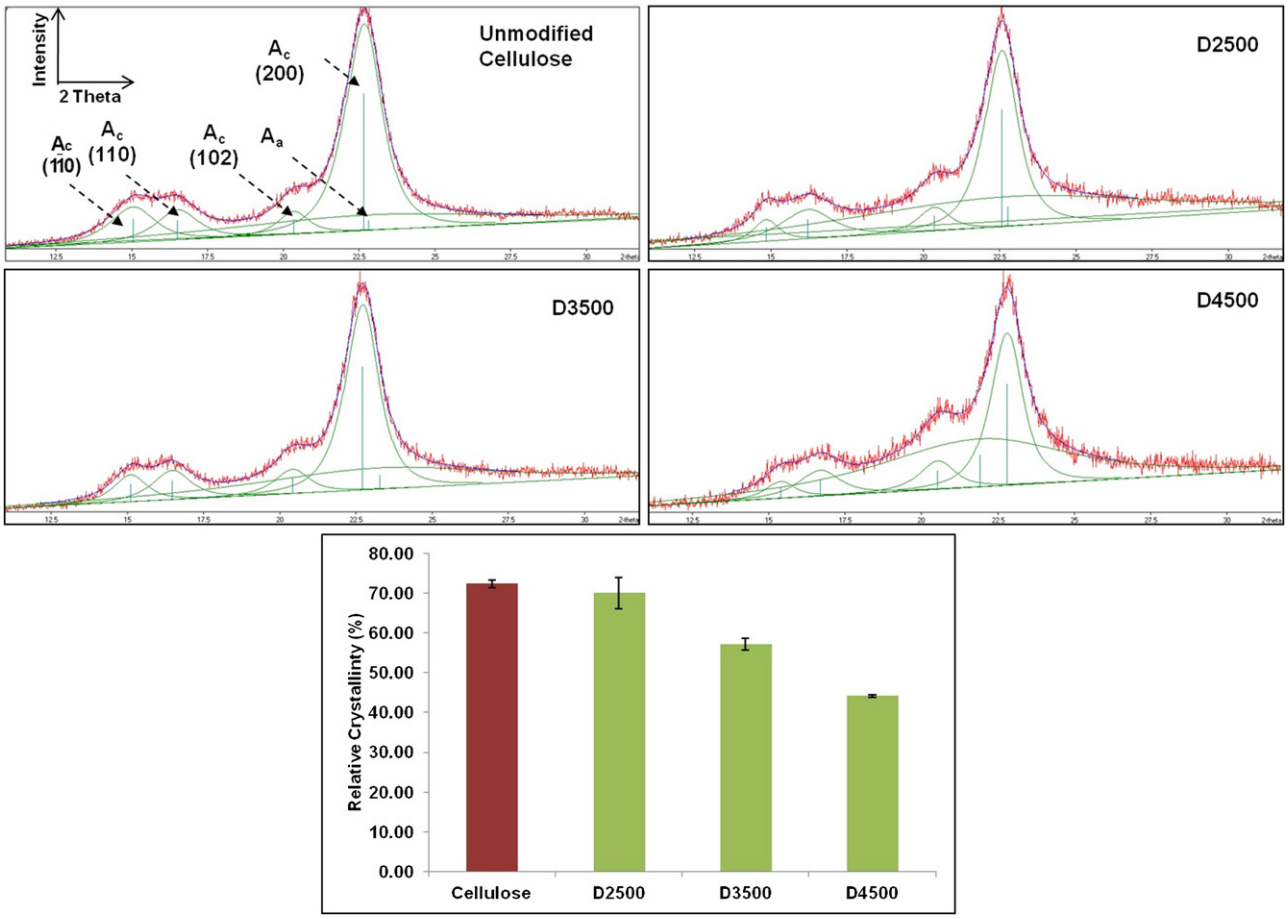

Fig. 3. Relative crystallinity of cellulose samples processed in DMSO and supercritical CO_2 at processing pressures 2500 psi, 3500 psi and 4500 psi.

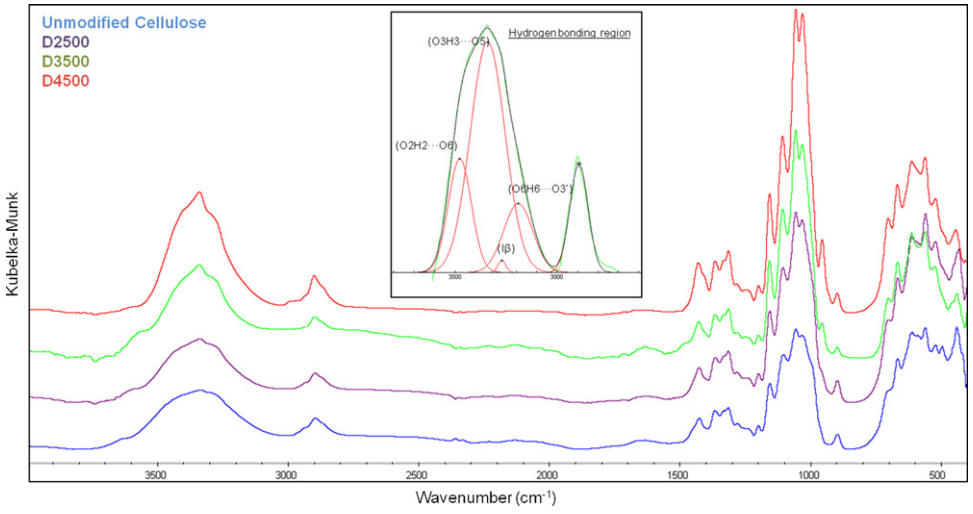

Fig. 4. DRIFT spectra of microcrystalline cellulose Avicel® FD100, D2500, D3500 and D4500 (bottom to top).

Table 4
Inter-chain and Intra-chain hydrogen bonds in Cellulose.

Wavenumber	Peak assignment in this work	Hydrogen bond type	References
3478	O2H2···O6	Intra-chain	Maréchal and Chanzy (2000)
3345	O3H3···O5	Intra-chain	Maréchal and Chanzy (2000), Kokot et al. (2002)
3208	O6H6···O3′	Inter-chain	Oh et al. (2005)
3274	Iβ	Hydrogen bond	Sugiyama et al. (1991)

Table 5
Change in wavenumber shift and peak height (intensity) of D2500, D3500 and D4500 samples relative to unmodified cellulose.

Hydrogen bond	Unmodified cellulose	D2500	D3500	D4500
O2H2···O6	3478	3451	3426	3417
Wavenumber shift	N/A	(−27)	(−52)	(−61)
O3H3···O5	3345	3353	3345	3345
Wavenumber shift	N/A	(+8)	(0)	(0)
O6H6···O3′	3208	3278	3298	3292
Wavenumber shift	N/A	(+70)	(+90)	(+90)
Iβ	3274	3274	3278	3274
Wavenumber shift	N/A	(0)	(+4)	(0)

Hydrogen bond	Peak height			
	Unmodified cellulose	D2500	D3500	D4500
O2H2···O6	0.01	0.03	0.03	0.05
O3H3···O5	0.04	0.02	0.03	0.03
O6H6···O3′	0.02	0.03	0.03	0.07

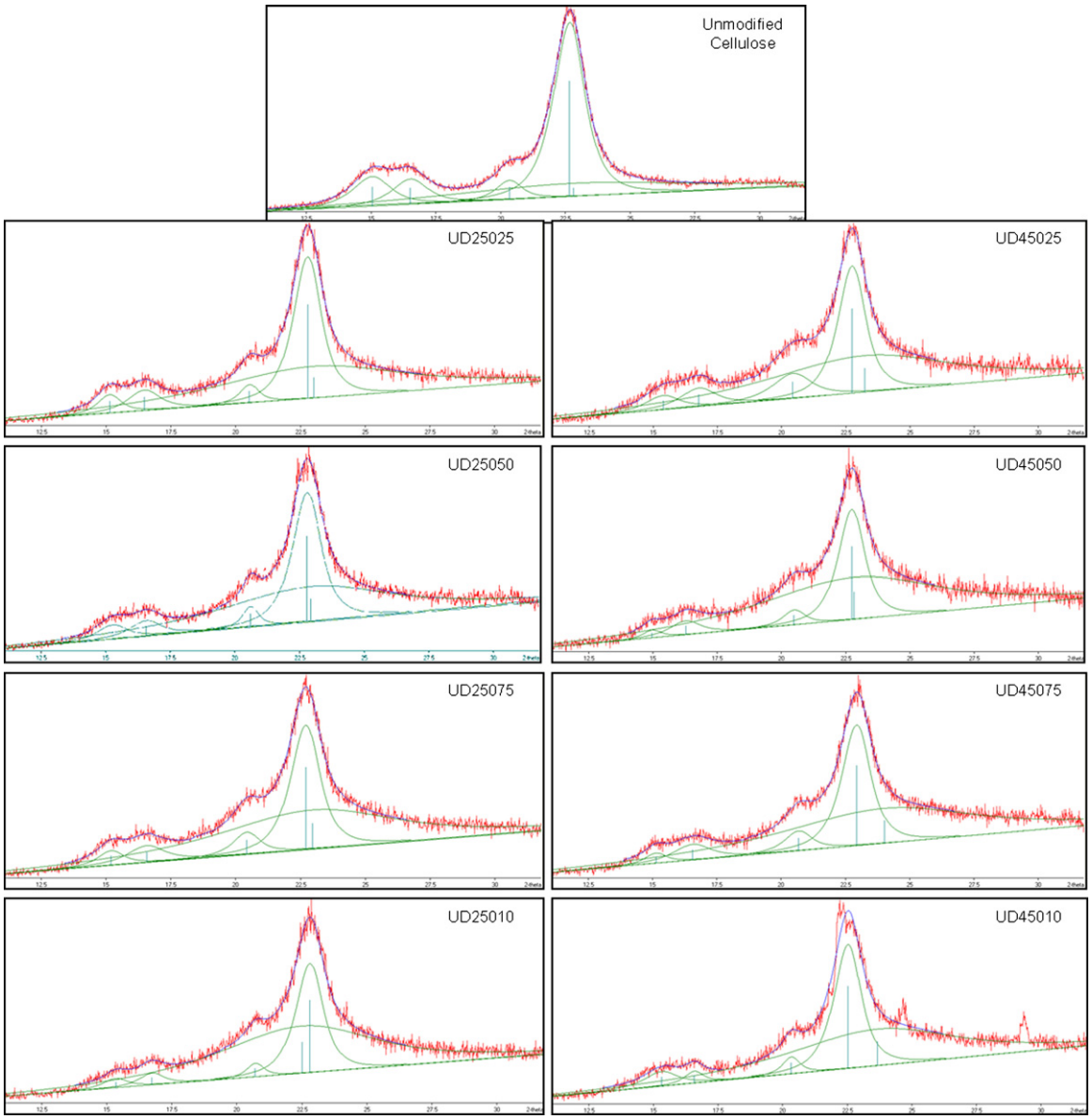

Fig. 5. WAXRD spectra of cellulose samples processed in DMSO–urea mixtures at 2500 psi and 4500 psi supercritical CO_2 pressures.

strength of inter-chain and intra-chain hydrogen bonding networks of cellulose due to processing. Peak deconvolution in the hydrogen-bonding region resulted in four individual spectral bands (Fig. 4, inset), which were assigned to inter-chain, and intra-chain hydrogen bonds in sample D2500 as listed in Table 4. Wavenumbers related to hydrogen bonds in cellulose shifted due to processing. These shifts relative to the hydrogen bonds in unmodified cellulose are listed in Table 5. In order to study the effect of processing on hydrogen bond intensity, peak heights of processed samples were compared with that of unmodified cellulose (Table 5).

It is known that among different hydrogen bonded hydroxyl groups, the one with stronger hydrogen bond is shifted more toward lower wavenumber in the spectrum (Maréchal & Chanzy, 2000). In comparison with unmodified cellulose, the movement of intra-chain hydrogen bond O2H2···O6 to lower wavenumbers and inter-chain hydrogen bond O6H6···O3′ to higher wavenumbers suggests strengthening of the O2H2···O6 and weakening of the O6H6···O3′ when supercritical CO_2 processing pressure is increased. It is also observed that processing pressures higher than 2500 psi caused significant reduction in O3H3···O5 bond intensity whereas the O6H6···O3′ bond intensity increased over unmodified cellulose. This might be possible that the increase in absorption intensity was caused by an increase in dipole moment due to interaction of DMSO molecules. This suggests that the DMSO + supercritical CO_2 preferentially interact with the inter-chain hydrogen bonds O6H6···O3′ and intra-chain hydrogen bonds O2H2···O6 but the degree of interaction changes for the intra-chain hydrogen bond at different levels of processing pressures, whereas it remains the same for inter-chain hydrogen bond for any level of supercritical CO_2 pressures studied herein. Fig. 4 also shows spectral changes at around 1035 cm^{-1} and 957 cm^{-1} for the cellulose samples processed in DMSO at different CO_2 pressures. The band at 1035 cm^{-1} is assigned to CH_3 rocking mode in DMSO (Skripkin et al., 2004) which is overlapped with the stretching vibrations of C6—O6 bond in cellulose (Oh et al., 2005). This band is found to match the intensity of stretching vibrations of C3—O3 (1058 cm^{-1}) in cellulose for D4500. This also suggests that DMSO molecules sterically interact with C6—O6 bond and change the environment around C6 carbon atom of cellulose to make this bond more polar. Cellulose processed under DMSO and supercritical CO_2 also shows two spectral bands at 957 cm^{-1} and 700 cm^{-1} from S=O stretching, CH_3 rocking combination, and asymmetric stretching vibrations of DMSO dimers respectively (Fawcett & Kloss, 1996; Martens, Frost, Kristof, & Theo Kloprogge, 2002; Skripkin et al., 2004). The increase in peak intensity at 957 cm^{-1} and narrowing of peak at 700 cm^{-1} with increase in CO_2 processing pressures suggest that the DMSO molecules were penetrating deeper into the crystalline structure of the cellulose.

From the above observations, it can be concluded that processing under DMSO and supercritical CO_2 at different pressures caused weakening of O6H6···O3′ inter-chain hydrogen bond yet all the hydroxyl groups still participate in forming hydrogen bond network such that overall hydrogen bond strength becomes and remains smaller than unmodified cellulose. Higher CO_2 pressure caused DMSO molecules penetrate deeper into crystalline structure of cellulose and interact mainly with O6H6···O3′ inter-chain hydrogen bond.

5.2. Microcrystalline cellulose processed with DMSO–urea–supercritical CO_2

5.2.1. WAXRD analysis

WAXRD spectra of samples with 0.25–1.00 g of urea in cellulose, processed with DMSO and supercritical CO_2 at 2500 psi and 4500 psi are shown in Fig. 5. It was found that crystal structure of cellulose mostly remained unchanged except that (2 0 0) peak intensity of all processed samples was reduced relative to unmodified cellulose. Some additional structural changes for the samples UD25010 and UD45010 were observed. In those samples, the intensity of planes (1 $\bar{1}$ 0) and (1 1 0) were relatively reduced and UD45010 showed some additional peaks at larger 2θ angles. These changes must be due to interference of excess urea particles. The amorphous region in urea containing cellulose samples was significantly larger than the unmodified cellulose. However, the amorphous region did not change significantly with either increase in urea content or variation in processing pressure. A quantitative comparison (Fig. 6) shows that the relative crystallinity of the sample UD25010 reduced as much as 50% from that of unmodified cellulose. However, the relative crystallinity of other urea containing cellulose samples formed a plateau at about 45%, which was similar to the cellulose processed without urea at 4500 psi. Overall, the relative degree of crystallinity did not change significantly as a function of urea content or pressure when urea was incorporated.

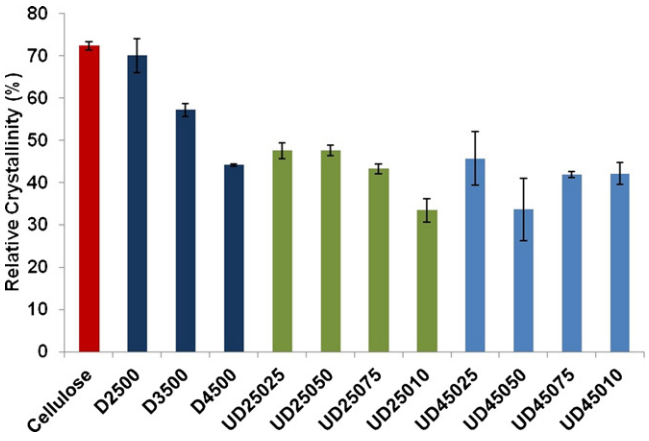

Fig. 6. Relative crystallinity of cellulose samples processed in DMSO and DMSO–urea mixture with supercritical CO_2.

Table 6
Peak assignments for hydrogen bonds in cellulose samples processed with DMSO/urea/supercritical CO_2.

Wavenumber (cm^{-1})	Peak assignment in this work	Hydrogen bond type
3454	O2H2···O6	Intra-chain
3371	O3H3···O5	Intra-chain
3248	O6H6···O3′	Inter-chain
3339	DMSO–urea complex	N/A
3200	DMSO–urea complex	N/A

5.2.2. DRIFT analysis

Cellulose samples processed in DMSO–urea mixture with supercritical CO_2 at 2500 psi and 4500 psi were characterized by DRIFT in order to understand the interactions between components and reason for limited reduction in relative crystallinity of cellulose. The sample with the highest molar ratio of urea to cellulose was chosen to assign the peaks to respective molecular bond vibrations. Fig. 7 inset shows deconvoluted hydrogen bonding region in IR spectra of UD25010. In comparison with hydrogen bonding region of unmodified cellulose, UD25010 includes an additional peak at around 3200 cm^{-1} which was formed due to presence of NH stretching vibrations (Mishra et al., 2006). Spectral bands around 3450 cm^{-1}, 3370 cm^{-1} and 3245 cm^{-1} were assigned to two intra-chain bonds O2H2···O6, O3H3···O5 and inter-chain hydrogen bond O6H6···O3′ respectively. A DMSO–urea complex was formed when urea was dissolved in DMSO; peaks at around 3340 cm^{-1} and 3200 cm^{-1} are assigned to signals from these compounds (Markarian et al., 2004) (Table 6). It is worth to note that peaks around these

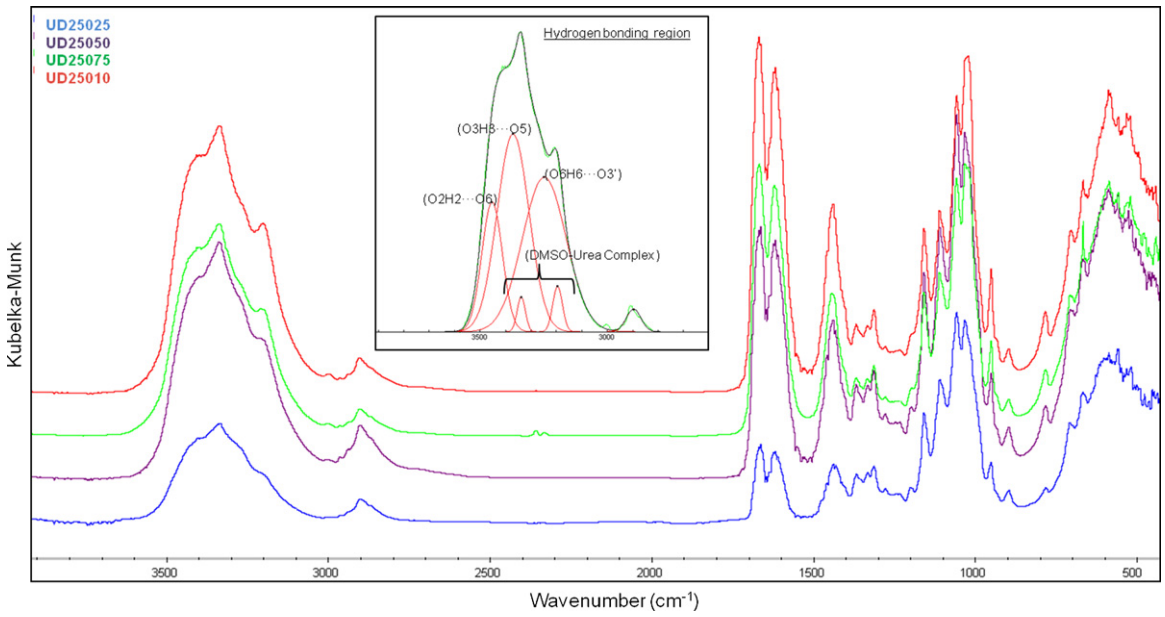

Fig. 7. DRIFT spectra of UD25025, UD25050, UD25075 and UD25010 (bottom to top).

wavenumbers were earlier assigned to intra-chain and inter-chain hydrogen bonds in unmodified cellulose. However, significant change in intensity and small shift of wavenumber corresponding to CH_2 bending (1430 cm^{-1}) suggests that DMSO–urea complex affects the environment around O6H6 bond; this resulted in spectral shift of band associated to inter-chain hydrogen bond O6H6···O3′. This observation provided a good reason to change the assignment for O6H6···O3′ from 3200 cm^{-1} to 3245 cm^{-1} for UD2500 and UD4500 samples. With a comparison to the IR spectra of unmodified cellulose, cellulose processed under DMSO–urea–supercritical CO_2 shows obvious new peaks in the range of 1600–1800 cm^{-1} which arise from C=O stretching vibrations of amide I (Mishra et al., 2006). The bands at 1620 cm^{-1} and 1670 cm^{-1} are assigned to ordered and disordered hydrogen bonded carbonyl groups respectively (Li et al., 2008; Yilgör, Burgaz, Yurtsever, & Yilgör, 2000). Asymmetric stretch of the H—C—N group in Urea was found at 1470 cm^{-1} (Liu, Yang, & Wang, 2007). This band is shifted to lower wavenumbers for processed samples due to weakening of its strength as a result of forming hydrogen bond with DMSO.

5.2.3. *Effect of urea concentration at CO_2 processing pressure of 2500 psi*

The FTIR spectra for the samples UD25025, UD25050, UD25075, and UD25010 are shown in Fig. 7. The hydrogen-bonding region (3200 cm^{-1} to 3600 cm^{-1}) in samples was deconvoluted by fityk software. The changes in wavenumber and intensity of peaks relative to corresponding peaks in unmodified cellulose are listed in Table 7. Intra-chain hydrogen bond O2H2···O6 shifted from 3478 cm^{-1} (unmodified cellulose) to around 3455 cm^{-1} for processed samples. However, it did not vary significantly among processed samples. On the other hand, spectral band of intra-chain hydrogen bond O3H3···O5 shifted to higher wavenumbers with increase in urea concentration. The spectral band for inter-chain hydrogen bond O6H6···O3′ also shifted to higher wavenumber for all the processed samples. The intensities of urea–DMSO complex were increased with increase in urea concentration. These observations suggest that processing caused reduction in the hydrogen bond strength of O3H3···O5 and O6H6···O3′ but increased the strength of O2H2···O6 in cellulose; this effect was more prominent in sample with highest urea content. Moreover, the spectral band at 1035 cm^{-1} was broadened and its ratio with spectral band at 1058 cm^{-1} increased by increase in urea content. As mentioned earlier, these bands are assigned to CH_3 rocking mode of DMSO (which is overlapped with C6H6···O6 of cellulose) and C3O3 of cellulose respectively. This shows incremental interaction of DMSO with C6H6···O6 of cellulose and more DMSO being trapped in cellulose with increase in urea content.

5.2.4. *Effect of urea concentration at CO_2 processing pressure of 4500 psi*

The FTIR spectra for samples UD45025, UD45050, UD45075, and UD45010 are shown in Fig. 8. Hydrogen bonding region in samples was deconvoluted by fityk software. The changes in wavenumber and intensity of peaks relative to corresponding peaks in unmodified cellulose are listed in Table 8. When compared to position of corresponding bands in unmodified cellulose, it was found that the spectral band for intra-chain hydrogen bond O2H2···O6 moved to lower wavenumbers and the band for O3H3···O5 was shifted to higher wavenumbers for UD45025 and UD45010 respectively. Moreover, the spectral band for inter-chain hydrogen bond O6H6···O3′ shifted to a higher wavenumber compared to that in unmodified cellulose. These observations suggest that processing resulted in weakening of hydrogen bonds O3H3···O5 and O6H6···O3′ whereas the bond O2H2···O6 was strengthened. Strengthening of O2H2···O6 can also be explained by reduction in its absorption intensity, which might be due to interaction of urea–DMSO complex preferentially with other two hydrogen bonds. However, the increase in urea content did not bring any significant difference in O6H6···O3′ inter-chain and O3H3···O5 intra-chain bond strengths for the two samples studied herein. The intensities for urea–DMSO complex increased for the sample containing higher amounts of urea. Also, the spectral band at 1035 cm^{-1} was broadened and its ratio with spectral band at 1058 cm^{-1} matched by increase in urea content. This shows interaction of DMSO with C6H6···O6 of cellulose increased and more DMSO was trapped in cellulose when urea content was increased.

From the above analysis, it can be concluded that addition of urea caused weakening of O3H3···O5 intra-chain hydrogen bond in addition to weakening of the inter-chain hydrogen bond unlike non-urea containing systems in which only the inter-chain hydrogen bond was weakened. This could imply slightly lower

Table 7
Change in wavenumber shift and peak height (intensity) of UD25025, UD25050, UD25075, UD2510 relative to unmodified cellulose.

Hydrogen bond	Unmodified cellulose	UD25025	UD25050	UD25075	UD25010
O2H2···O6	3478	3447	3454	3457	3454
Wavenumber shift	N/A	(−31)	(−24)	(−21)	(−24)
O3H3···O5	3345	3352	3360	3375	3371
Wavenumber shift	N/A	(+7)	(+15)	(+30)	(+26)
O6H6···O3′	3208	3255	3233	3235	3248
Wavenumber shift	N/A	(+47)	(+25)	(+27)	(+30)

Hydrogen bond	Peak height				
	Unmodified cellulose	UD25025	UD25050	UD25075	UD25010
O2H2···O6	0.01	0.02	0.16	0.20	0.21
O3H3···O5	0.04	0.02	0.27	0.11	0.26
O6H6···O3′	0.02	0.07	0.14	0.18	0.17

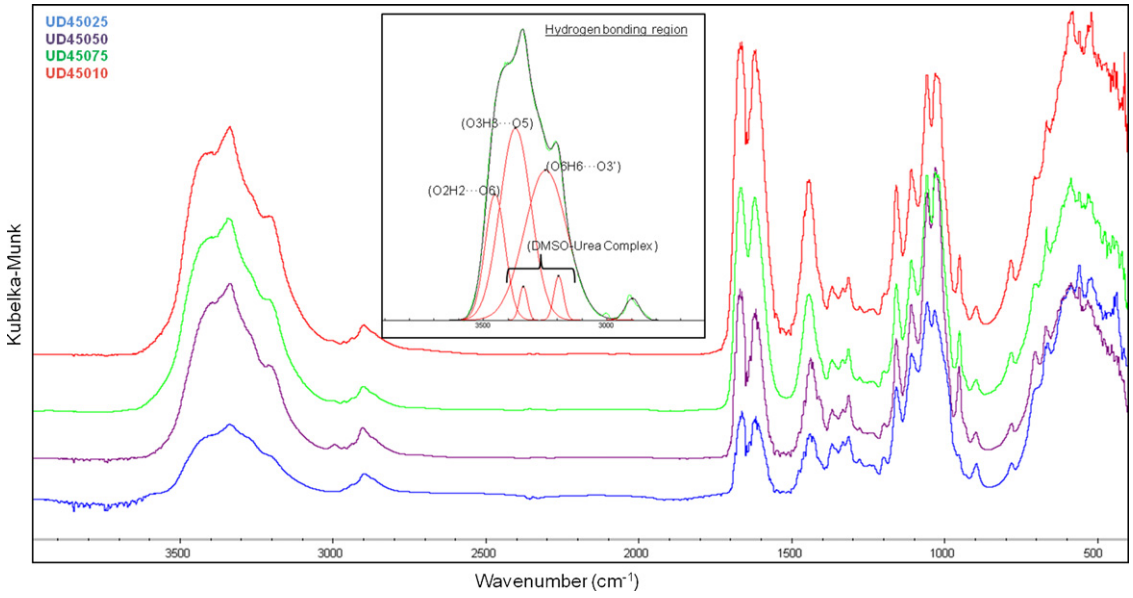

Fig. 8. DRIFT spectra of UD45025, UD45050, UD45075 and UD45010 (bottom to top).

Table 8
Change in wavenumber shift and peak height (intensity) of UD45025, UD45050, UD45075, UD4510 relative to unmodified cellulose.

Hydrogen bond	Unmodified cellulose	UD45025	UD45050	UD45075	UD45010
O2H2···O6	3478	3454	3444	3461	3460
Wavenumber shift	N/A	(−24)	(−34)	(−17)	(−18)
O3H3···O5	3345	3357	3343	3389	3387
Wavenumber shift	N/A	(+12)	(−2)	(+44)	(+42)
O6H6···O3′	3208	3245	3211	3242	3244
Wavenumber shift	N/A	(+37)	(+3)	(+34)	(+36)

Hydrogen bond	Peak height				
	Unmodified cellulose	UD45025	UD45050	UD45075	UD45010
O2H2···O6	0.01	0.03	0.08	0.12	0.16
O3H3···O5	0.04	0.05	0.19	0.22	0.24
O6H6···O3′	0.02	0.03	0.12	0.06	0.10

crystallinity of cellulose samples that contains urea. However, change in hydrogen bonding was also due to presence of urea–DMSO complex that was entrapped in cellulose after processing. The DMSO–urea complex reduced the solubility of DMSO in supercritical CO_2 and retained more DMSO–urea complex trapped inside microfibrils of cellulose after depressurization process. Dissolution of urea in DMSO prevented the direct interaction with cellulose. Therefore, increase in urea content did not bring any considerable change in molecular bond strength and hence the crystallinity of cellulose samples did not show a significant change by varying urea content.

6. Conclusion

In this work, a method to partially reduce the crystallinity of cellulose using a combination of solvents viz. DMSO and DMSO–urea

mixture with supercritical CO_2 was developed. Microcrystalline cellulose was first solvated with DMSO (or DMSO–urea mixture) and pressurized using supercritical CO_2 at various pressures. DMSO was finally extracted and cellulose was collected in a dry powder form. The effect of processing microcrystalline cellulose in DMSO, urea, and supercritical CO_2 was studied. Processing under DMSO (and urea) with supercritical CO_2 did not break the crystalline regions of microcrystalline cellulose completely. Yet the experiments resulted in significant reduction of the relative crystallinity, which mostly occurred due to the plasticization of short-range order – amorphous regions in cellulose. Processing of microcrystalline cellulose with DMSO (or DMSO–urea mixture) with supercritical CO_2 caused restructuring of inter-chain and intra-chain hydrogen bonding in cellulose. For cellulose without urea, DMSO molecules primarily interacted around the O2H2···O6 intra-chain hydrogen bond which, in presence of supercritical CO_2, resulted in stretching and weakening of the O6H6···O3′ inter-chain hydrogen bond. In samples of cellulose with urea, the DMSO–urea complex with supercritical CO_2 caused weakening of O3H3···O5 intra-chain as well as O6H6···O3′ inter-chain hydrogen bond. Increase in supercritical CO_2 pressure resulted in deeper penetration of DMSO in cellulose. For urea containing cellulose samples, extraction of DMSO during CO_2 depressurization was affected by presence of urea.

Acknowledgements

We are grateful to Dr. Kirk Ziegler from Department of Chemical Engineering, University of Florida for lending us the view cell to conduct batch-processing experiments. We are also thankful to staff at Particle Engineering and Research Center, University of Florida to provide necessary instrumental support.

References

Aminabhavi, T. M., & Gopalakrishna, B. (1995). Density, viscosity, refractive index, and speed of sound in aqueous mixtures of N,N-dimethylformamide, dimethyl sulfoxide, N,N-dimethylacetamide, acetonitrile, ethylene glycol, diethylene glycol, 1,4-dioxane, tetrahydrofuran, 2-methoxyethanol, and 2-ethoxyethanol at 298.15 K. *Journal of Chemical & Engineering Data*, *40*(4), 856–861.

Bansal, P., Hall, M., Realff, M. J., Lee, J. H., & Bommarius, A. S. (2010). Multivariate statistical analysis of X-ray data from cellulose: A new method to determine degree of crystallinity and predict hydrolysis rates. *Bioresource Technology*, *101*(12), 4461–4471.

Briassoulis, D. (2004). An overview on the mechanical behaviour of biodegradable agricultural films. *Journal of Polymers and the Environment*, *12*(2), 65–81.

Catchpole, O. J., Tallon, S. J., Dyer, P. J., Lan, J. S., Jensen, B., Rasmussen, O. K., et al. (2005). Measurement and modelling of urea solubility in supercritical CO_2 and CO_2 + ethanol mixtures. *Fluid Phase Equilibria*, *237*(1–2), 212–218.

Edgar, K. J., Buchanan, C. M., Debenham, J. S., Rundquist, P. A., Seiler, B. D., Shelton, M. C., et al. (2001). Advances in cellulose ester performance and application. *Progress in Polymer Science*, *26*, 1605–1688.

Fawcett, W. R., & Kloss, A. A. (1996). Attenuated total reflection Fourier-transform IR spectroscopic study of dimethyl sulfoxide self-association in acetonitrile solutions. *Journal of the Chemical Society, Faraday Transactions*, *92*(18), 3333–3337.

Fernandez Cid, M. V., Gerstner, K. N., van Spronsen, J., van der Kraan, M., Veugelers, W. J. T., Woerlee, G. F., et al. (2007). Novel process to enhance the dyeability of cotton in supercritical carbon dioxide. *Textile Research Journal*, *77*(1), 38–46.

Focher, B., Palma, M. T., Canetti, M., Torri, G., Cosentino, C., & Gastaldi, G. (2001). Structural differences between non-wood plant celluloses: Evidence from solid state NMR, vibrational spectroscopy and X-ray diffractometry. *Industrial Crops and Products*, *13*(3), 193–208.

Garvey, C. J., Parker, I. H., & Simon, G. P. (2005). On the interpretation of X-ray diffraction powder patterns in terms of the nanostructure of cellulose I fibres. *Macromolecular Chemistry and Physics*, *206*(15), 1568–1575.

Ilharco, L. M., Garcia, A. R., Lopes da Silva, J., & Vieira Ferreira, L. F. (1997). Infrared approach to the study of adsorption on cellulose: Influence of cellulose crystallinity on the adsorption of benzophenone. *Langmuir*, *13*(15), 4126–4132.

Johnston, K. P., & Shah, P. S. (2004). Making nanoscale materials with supercritical fluids. *Science*, *303*(5657), 482–483.

Kazarian, S. G. (2000). Polymer processing with supercritical fluids. *Polymer Science Series C*, *42*(1), 78–101.

Kjellow, A. W., & Henriksen, O. (2009). Supercritical wood impregnation. *The Journal of Supercritical Fluids*, *50*(3), 297–304.

Klemm, D., Heublein, B., Fink, H.-P., & Bohn, A. (2005). Cellulose: Fascinating Biopolymer and Sustainable Raw Material. *Angewandte Chemie International Edition*, *44*(22), 3358–3393.

Klemm, D., Schmauder, H.-P., & Heinze, T. (2005). *Cellulose*. Jena, Germany: Wiley-VCH Verlag GmbH & Co. KGaA.

Kokot, S., Czarnik-Matusewicz, B., & Ozaki, Y. (2002). Two-dimensional correlation spectroscopy and principal component analysis studies of temperature-dependent IR spectra of cotton–cellulose. *Biopolymers*, *67*(6), 456–469.

Kondo, T., Sawatari, C., Manley, R. S. J., & Gray, D. G. (1994). Characterization of hydrogen bonding in cellulose-synthetic polymer blend systems with regioselectively substituted methylcellulose. *Macromolecules*, *27*(1), 210–215.

Kovalenko, V. I. (2010). Crystalline cellulose: structure and hydrogen bonds. *Russian Chemical Reviews*, *79*, 231.

Krässig, H. (1993). Cellulose: structure, accessibility, and reactivity. *Gordon and Breach Science*, *11*, 376.

Leitner, W. (1999). Reactions in supercritical carbon dioxide. In P. Knochel (Ed.), *Modern solvents in organic synthesis* (pp. 107–132). Berlin/Heidelberg: Springer.

Li, Z. F., Li, J. Y., Sun, J., Sun, B. Q., Wang, J. J., & Shen, Q. (2008). Investigation of kinetics and morphology development for polyurethane–urea extended by DMTDA. *Frontiers of Materials Science in China*, *2*(2), 200–204.

Liu, J.-Y., Yang, C.-C., & Wang, Y.-Z. (2007). Miscibility and physical properties of conducting poly(urea-urethane) thermoplastic elastomers. *Journal of Applied Polymer Science*, *103*(6), 3803–3810.

Maréchal, Y., & Chanzy, H. (2000). The hydrogen bond network in I[beta] cellulose as observed by infrared spectrometry. *Journal of Molecular Structure*, *523*(1-3), 183–196.

Markarian, S. A., Gabrielyan, L. S., & Grigoryan, K. R. (2004). FT IR ATR study of molecular interactions in the urea/dimethyl sulfoxide and urea/diethyl sulfoxide binary systems. *Journal of Solution Chemistry*, *33*(8), 1005–1015.

Martens, W. N., Frost, R. L., Kristof, J., & Theo Kloprogge, J. (2002). Raman spectroscopy of dimethyl sulphoxide and deuterated dimethyl sulphoxide at 298 and 77 K. *Journal of Raman Spectroscopy*, *33*(2), 84–91.

Mishra, A. K., Chattopadhyay, D. K., Sreedhar, B., & Raju, K. V. S. N. (2006). FT-IR and XPS studies of polyurethane–urea-imide coatings. *Progress in Organic Coatings*, *55*(3), 231–243.

Nada, A.-A. M. A., Kamel, S., & El-Sakhawy, M. (2000). Thermal behaviour and infrared spectroscopy of cellulose carbamates. *Polymer Degradation and Stability*, *70*(3), 347–355.

O'Sullivan, A. (1997). Cellulose: the structure slowly unravels. *Cellulose*, *4*(3), 173–207.

Oh, S. Y., Yoo, D. I., Shin, Y., Kim, H. C., Kim, H. Y., Chung, Y. S., et al. (2005). Crystalline structure analysis of cellulose treated with sodium hydroxide and carbon dioxide by means of X-ray diffraction and FTIR spectroscopy. *Carbohydrate Research*, *340*(15), 2376–2391.

Park, S., Baker, J., Himmel, M., Parilla, P., & Johnson, D. (2010). Cellulose crystallinity index: Measurement techniques and their impact on interpreting cellulase performance. *Biotechnology for Biofuels*, *3*(1), 10.

Rajasingam, R., Lioe, L., Pham, Q. T., & Lucien, F. P. (2004). Solubility of carbon dioxide in dimethylsulfoxide and N-methyl-2-pyrrolidone at elevated pressure. *The Journal of Supercritical Fluids*, *31*(3), 227–234.

Schacht, C., Zetzl, C., & Brunner, G. (2008). From plant materials to ethanol by means of supercritical fluid technology. *The Journal of Supercritical Fluids*, *46*(3), 299–321.

Scott, G. (2002). *Degradable polymers: Principles and applications*. Jena, Germany: Kluwer Academic Publishers.

Skripkin, M. Y., Lindqvist-Reis, P., Abbasi, A., Mink, J., Persson, I., & Sandstrom, M. (2004). Vibrational spectroscopic force field studies of dimethyl sulfoxide and hexakis(dimethyl sulfoxide)scandium(iii) iodide, and crystal and solution structure of the hexakis(dimethyl sulfoxide)scandium(iii) ion. *Dalton Transactions*, (23), 4038–4049.

Sugiyama, J., Persson, J., & Chanzy, H. (1991). Combined infrared and electron diffraction study of the polymorphism of native celluloses. *Macromolecules*, *24*(9), 2461–2466.

Taherzadeh, M., & Karimi, K. (2008). Pretreatment of lignocellulosic wastes to improve ethanol and biogas production: A review. *International Journal of Molecular Sciences*, *9*(9), 1621–1651.

Vega Gonzalez, A., Tufeu, R., & Subra, P. (2002). High-pressure vapor–liquid equilibrium for the binary systems carbon dioxide + dimethyl sulfoxide and carbon dioxide + dichloromethane. *Journal of Chemical & Engineering Data*, *47*(3), 492–495.

Watanabe, A., Morita, S., & Ozaki, Y. (2006). Study on temperature-dependent changes in hydrogen bonds in cellulose Iβ by infrared spectroscopy with perturbation-correlation moving-window two-dimensional correlation spectroscopy. *Biomacromolecules*, *7*(11), 3164–3170.

Wen, D., Jiang, H., & Zhang, K. (2009). Supercritical fluids technology for clean biofuel production. *Progress in Natural Science*, *19*(3), 273–284.

Wypych, G. (2001). *Handbook of solvents*. Jena, Germany: ChemTec.

Yilgör, E., Burgaz, E., Yurtsever, E., & Yilgör, I. (2000). Comparison of hydrogen bonding in polydimethylsiloxane and polyether based urethane and urea copolymers. *Polymer*, *41*(3), 849–857.

Yin, C., Li, J., Xu, Q., Peng, Q., Liu, Y., & Shen, X. (2007). Chemical modification of cotton cellulose in supercritical carbon dioxide: Synthesis and characterization of cellulose carbamate. *Carbohydrate Polymers*, *67*(2), 147–154.

Zhang, J., Zhang, J., Lin, L., Chen, T., Zhang, J., Liu, S., et al. (2009). Dissolution of microcrystalline cellulose in phosphoric acid—molecular changes and kinetics. *Molecules*, *14*(12), 5027–5041.
Zheng, Y., Lin, H. M., & Tsao, G. T. (1998). Pretreatment for cellulose hydrolysis by carbon dioxide explosion. *Biotechnology Progress*, *14*(6), 890–896.
Zheng, Y., & Tsao, G. T. (1996). Avicel hydrolysis by cellulase enzyme in supercritical CO_2. *Biotechnology Letters*, *18*(4), 451–454.
Zhou, D., Zhang, L., & Guo, S. (2005). Mechanisms of lead biosorption on cellulose/chitin beads. *Water Research*, *39*(16), 3755–3762.